

Flux-Pumped Josephson Travelling-Wave Parametric Amplifiers Based on Bi-SQUID Cells

Renat A. Yusupov , Lyudmila V. Filippenko, Daniil E. Bazulin, Nikolay V. Kolotinskiy , *Member, IEEE*,
Mikhail A. Tarasov , Edward Goldobin, Valery P. Koshelets , *Member, IEEE*,
and Victor K. Kornev , *Member, IEEE*

Abstract—We have proposed a new design of the Josephson traveling-wave parametric amplifier (JTWPA) capable of providing much higher spurious-free dynamic range (SFDR). For this purpose, we substitute dc SQUIDs for bi-SQUIDs in the used artificial signal transmission line driven by external travelling-wave magnetic flux. The increase of SFDR follows from the increased linearity domain of the phase-current relation in bi-SQUID as compared to dc SQUID. Optimal parameters for bi-SQUIDs have been determined. The first version of JTWPA was modeled to be fabricated using niobium process.

Index Terms—Artificial microwave transmission line, bi-SQUID, current-phase relation, dc SQUID, dynamic range, Josephson traveling wave parametric amplifier, linearity, 3-wave signal mixing mode.

I. INTRODUCTION

JOSEPHSON Traveling-Wave Parametric Amplifiers (JTWPA) with ultimately low internal noise are currently considered as promising devices for use in the field of precision quantum measurements (including single-photon detectors), quantum communications and quantum computing. Moreover, the amplifiers are free from the gain-bandwidth tradeoff, which is inherent in the conventional cavity-based parametric amplifiers. All the proposed designs are based on the use of an

Manuscript received September 29, 2021; revised November 15, 2021; accepted November 19, 2021. Date of publication November 26, 2021; date of current version December 30, 2021. This work was supported by the Russian Science Foundation under Project no. 21-42-04421. The modeling of bi-SQUID was carried out under a grant from the Russian Science Foundation (Project no. 19-72-10016). The equipment of USU “Cryointegral” was used to carry out the research; USU is supported by a grant from the Ministry of Science and Higher Education of the Russian Federation, Agreement no. 075-15-2021-667. (Corresponding author: Renat A. Yusupov.)

Renat A. Yusupov, Lyudmila V. Filippenko, Mikhail A. Tarasov, and Valery P. Koshelets are with the Laboratory of superconduction devices for signal detection and processing, Kotelnikov Institute of Radio Engineering and Electronics of RAS, 125009 Moscow, Russia (e-mail: yusupovrenat@hitech.cplire.ru).

Daniil E. Bazulin is with the Faculty of Physics, Lomonosov Moscow State University, 119991 Moscow, Russia, and also with Walther-Meißner-Institut, Bayerische Akademie der Wissenschaften, 85748, Garching, Germany.

Nikolay V. Kolotinskiy is with the Quantum Technology Centre, Lomonosov Moscow State University, 119991 Moscow, Russia.

Edward Goldobin is with the Physics Institute – Experimental Physics II, 72076 Tübingen, Germany (e-mail: gold@uni-tuebingen.de).

Victor K. Kornev is with the Faculty of Physics, Lomonosov Moscow State University, 119991 Moscow, Russia (e-mail: kornev@phys.msu.ru).

Color versions of one or more figures in this article are available at <https://doi.org/10.1109/TASC.2021.3131134>.

Digital Object Identifier 10.1109/TASC.2021.3131134

artificial microwave transmission line comprising a series chain of cells with nonlinear Josephson inductances [1]–[13]. The favorable 3-wave mixing mode can be realized with the cells in the form of either rf or dc SQUIDs [7]–[11]. This mode is free from the self- and cross-modulation effects in contrast to the 4-wave one.

In developing the most optimal JTWPA design, the challenging task is to combine the extremely high sensitivity with both the high signal gain and high dynamic range free from nonlinear distortions. For this purpose, an individual transmission line for the pump signal has been suggested [11] to eliminate the pump wave depletion that strongly limits signal gain and dynamic range of the single-line JTWPA [7], [8]. The use of such a dedicated line inductively coupled to the signal transmission line cells removes restriction on power of the pump wave and enables the required uniform traveling wave modulation of the cell inductances.

Further improvement of the device characteristics can be obtained with increasing linearity of the phase-current relation in the cells of the signal transmission line. As shown in [11] for JTWPA with the signal transmission line composed of dc SQUIDs, such a linear relation between the current flowing through the cell and Josephson phase drop on the cell yields in linear wave equation (in continuum approximation) with spatial time-varying inductive parameter. Thus, both the signal and idler waves propagate with amplification in linear regime, while the wave transport current I_b is much less than the maximum superconducting current of the cells (i.e. the device acts as a linear amplifier at fixed number of the cells), otherwise the unwanted nonlinear regime occurs.

An increase in the critical current I_c of the used Josephson junctions cannot be an acceptable solution for extending the linear domain, since the increase of I_c decreases the characteristic value $L_{J0} = \Phi_0 / (2\pi I_c)$ of the Josephson-junction inductance (where $\Phi_0 = h/(2e)$ is the magnetic flux quantum) enabled for the time-varying modulation by the pump wave. As far as the effective cell inductance L_{eff} assigns ratio of the specified wave impedance $z_0 = \sqrt{L_{cell}/C}$ to the cutoff frequency $\omega_{cr} = 1/\sqrt{L_{cell}C}$ (where C is the ground capacitance per cell), z_0/ω_{cr} , the decrease of L_{J0} , and hence of L_{cell} , raises the cutoff frequency and thereby reduces gain factor as shown in [11]. Of course, the decrease in L_{J0} can be compensated through increase in geometric inductance of the cells to fix the cutoff frequency,

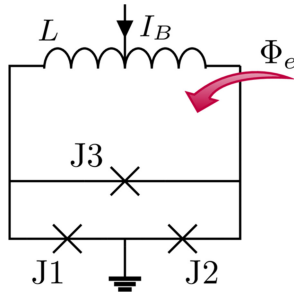


Fig. 1. Schematic of a bi-SQUID suggested to linearize the dc SQUID voltage response function [9]. The introduced additional Josephson junction J3 is connected in parallel with the main (geometric) inductance L . The other geometric inductances (existing in the 3-junction loop) ought to be reasonably low [10] and therefore are not shown.

but this measure reduces the available modulation depth m of the cell inductance L_{cell} and hence decreases the gain factor as well [11]. Thus, one should pay attention to the type and design of the cells in use.

In this paper, we propose using bi-SQUIDs as cells of the signal transmission line of JTWPA to improve linearity of the cell characteristics and hence increase spurious-free dynamic range (SFDR) of the amplifier. The parametric amplifier is to be fabricated using niobium process.

II. ARCHITECTURE OF BI-SQUID BASED JTWPA

Bi-SQUID was suggested initially [16] to linearize the dc SQUID voltage response function by implementing two successive nonlinear signal transformations, which are to be tuned to mutually inverse form. For this purpose, an additional Josephson junction is connected in parallel to the main (geometric) inductance of the two-junction SQUID as shown in Fig. 1. In the device, the applied magnetic flux Φ_e is transformed first to Josephson phase of the third junction and then to output voltage. At properly assigned parameters, the resulting voltage response dependence on the input magnetic flux can have either exactly triangular form when $l^* \equiv i_{c3}l = 1$ or hysteretic triangular-like one when $l^* > 1$ [17], [18], where

$$i_{c3} = I_{c3} / I_c, \quad (1)$$

$$l = 2\pi I_c L / \Phi_0, \quad (2)$$

I_{c3} and I_c are critical currents of the third Josephson junction and the base junctions J1, J2, respectively, L is the main (geometric) inductance of the device.

Though the bi-SQUID developing was aimed at its use just in resistive state, the additional degree of freedom appeared with adding the third Josephson junction enables tuning characteristics of the device in superconducting state as well. In particular, linearity of the relation between transport current I_b (total current of the signal and idler waves in the amplifier) and the Josephson phase drop on bi-SQUID can be considerably improved and extended to much higher magnitude of the current. As shown below, one can be aimed at the following parameter domains: $i_{c3} \simeq 1.5$ to 2 together with $l \simeq 0.25$ to 1.

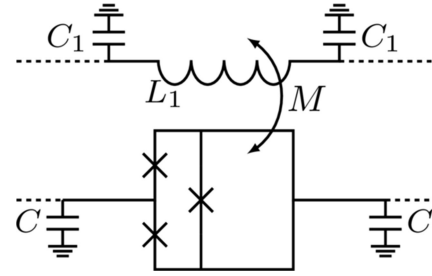


Fig. 2. Inductively-coupled elementary cells in the pump and signal transmission lines of JTWPA based on using bi-SQUIDs. C , C_1 are ground capacitances of the lines.

Fig. 2 shows schematically segment of the JTWPA based on using bi-SQUIDs as unit cells of the signal transmission line coupled inductively with cells of the separate pump line. In general, the circuit corresponds to the amplifier architecture proposed recently by A. Zorin [11], however with replacement of dc SQUIDs by bi-SQUIDs. In the case of sufficiently small coupling, when $\kappa = M/L_1 \ll 1$, and sufficiently large power P_p of the pump wave, the pump signal remains undepleted and provides a traveling flux wave with the constant amplitude $\Phi_{p0} \propto \sqrt{P_p}$. The flux modulates magnitude of the maximum superconducting currents of bi-SQUIDs and hence causes the differential inductance of the cells $L_{cell} \equiv L_d = d(\Delta\varphi\Phi_0/2\pi)/dI_b$ to vary in the wave manner [11]:

$$L_d^{-1} = L_{d0}^{-1} (1 + m \cdot \sin(k_p x - \omega_p t)), \quad (3)$$

enabling parametric amplification. In the formula, $\Delta\varphi$ is the Josephson phase dropped on the cell, the coordinate x is normalized on the cell size, the modulation depth $m \propto \Phi_{p0}$, and the magnitude L_{d0} is assigned by applying dc magnetic flux Φ_{dc} , e. g. $\sim \Phi_0/3$ as was recommended in [11].

One should emphasize the fact that in such a flux-pumped JTWPA the mixing capabilities of the medium are to be given only by the straightforward modulation of its reactive (inductive) parameter induced by the rf component of the external flux drive and not on the cell non-linearity, as it happens in non-flux-pumped SQUID-based JTWPA (e.g. see [7], [8]). Nevertheless, although the cell non-linearity is unwanted in the flux-pumped amplifiers, some nonlinearity of the phase-current relation $\Delta\varphi(I_b)$ appears inevitably with increase of the transport current I_b (produced by both the signal and idler waves) causing a reduction of the dynamic range of the amplifier. Therefore, the reduced non-linearity of the bi-SQUID cells will increase the gain compression point.

III. BI-SQUID VS. DC SQUID FOR JTWPA

In case of a slow-varying transport current I_b (when its frequency ω is much less than both the Josephson characteristic and plasma frequencies $\omega_c = 2\pi I_c R_n / \Phi_0$, $\omega_o = \sqrt{2\pi I_c / (\Phi_0 C_j)}$; C_j and R_n are the junction capacitance and normal resistance) flowing via a symmetric dc SQUID and a symmetric bi-SQUID both in superconducting state, Josephson phases φ_1 and φ_2 of the junctions J1 and J2 obey the current relation

$$i_b \equiv I_b / I_c = i_2 + i_1 = \sin\varphi_2 + \sin\varphi_1 \quad (4)$$

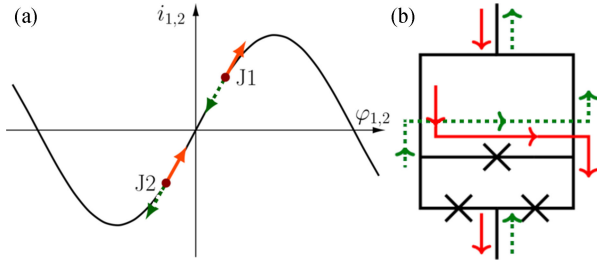


Fig. 3. (a) Josephson phases and currents through the junctions J1 and J2 described by two points in sinusoid on the current-phase plane when some dc magnetic flux is applied to the cell, dc SQUID or bi-SQUID, and transport current is absent. The red and green arrows show directions of displacement of the points at positive (red color) and negative (green dotted color) transport current. (b) Paths of the current flowing through the additional junction in bi-SQUID at positive (red lines and red arrows) and negative (green dotted lines and arrows) transport currents.

and the phase equation which is

$$\varphi_2 - \varphi_1 = \varphi_e - l(\sin \varphi_2 - \sin \varphi_1) / 2 \quad (5)$$

for dc SQUID and

$$\varphi_2 - \varphi_1 = \varphi_e - l(\sin \varphi_2 - \sin \varphi_1) / 2 - li_{c3} \sin(\varphi_2 - \varphi_1) \quad (6)$$

for bi-SQUID. In both equations, l is the normalized loop inductance (2), $\varphi_e = 2\pi\Phi_e/\Phi_0$ is normalized value of the applied magnetic flux $\Phi_e = \Phi_{dc} + \Phi_{rf}$, where Φ_{dc} is the applied dc magnetic flux, and Φ_{rf} is the rf magnetic flux which is applied by the pump wave; correspondingly, $\varphi_e = \varphi_{dc} + \varphi_{rf}$.

In the absence of both the signal and idler waves (when transport current $i_b = 0$), Josephson phases φ_1 and φ_2 of the junctions J1 and J2 in symmetric cells of both types, dc SQUID and bi-SQUID, are equal in magnitude and opposite in their signs in regard to direction of transport current, *i. e.* $\varphi_2 = -\varphi_1$. Fig. 3(a) shows schematically the phases and the currents flowing through the junctions J1 and J2 when the only dc magnetic flux is applied to dc SQUID or bi-SQUID. At negligibly small inductance l of the devices, as assumed in [11], $\varphi_1 = -\varphi_2 = \varphi_{dc} / 2$.

Transport current i_b produced by the signal and idler waves causes displacement of both the points 1 and 2 shown in Fig. 3(a) in the sinusoid in direction corresponding to either increase of the junction phases at $i_b > 0$ or decrease of the ones at $i_b < 0$, and some drop of Josephson phase $\Delta\varphi$ appears on the cell. Relation between the phase drop and the transport current is evidently nonlinear. As seen from the sketch (Fig. 3(a)), the nonlinearity results from either the first junction at positive transport current (corresponding to red color of the shown arrows) or the second junction (green arrows) at negative transport current.

The nonlinearity problem is considerably mitigated in bi-SQUID through the current flowing via the added Josephson junction J3. This current flows through the third junction always in the same direction independently on the transport current direction, however on different paths through the other circuit elements in dependence on the transport current direction and therefore changes division of the transport current between the main junctions J1 and J2. These two possible paths of the current I_3 are shown in Fig. 3(b) by the red lines and red arrows for the positive transport current and by the green lines and arrows for

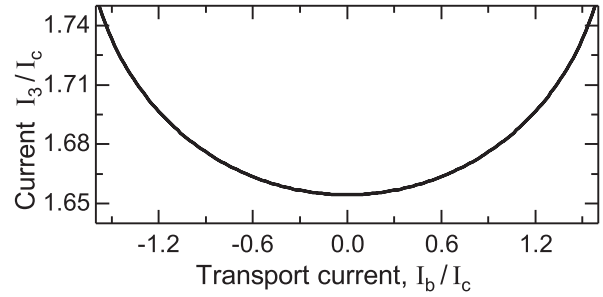


Fig. 4. Dependence of the current flowing in bi-SQUID through the 3rd Josephson junction on the transport current $i_b = I_b/I_c$ at $l = 0.5$, $i_{c3} = 2$, and $\varphi_{dc} = 2\pi/3$.

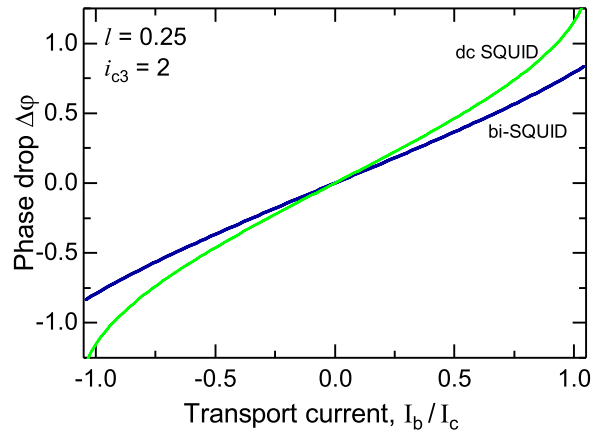


Fig. 5. Phase drops on both dc SQUID (green line) and bi-SQUID (blue line) with $i_{c3} = 2$ and same value $l = 0.25$ versus transport current. The same dc magnetic flux $\Phi_{dc} = \Phi_0/3$ is applied to both devices.

the negative transport current. In both cases, current I_3 provides decrease in the current flowing through that junction which is responsible for nonlinearity in the relation between the phase drop $\Delta\varphi$ and transport current i_b .

As an example, Fig. 4 shows dependence of the current $i_3 = I_3/I_c$ on the transport current $i_b = I_b/I_c$ at $l = 0.5$, $i_{c3} = 2$, and $\varphi_{dc} = 2\pi/3$. It should be noted that such a redistribution of the current becomes impossible at $l \rightarrow 0$, however, the value of the normalized geometric inductance $l \simeq 0.25$ to 1 is quite sufficient. The linearity improvement effect increases with an increase in the critical current I_{c3} of the third Josephson junction and becomes quite sufficient at $i_{c3} = I_{c3}/I_c \simeq 1.5$ to 2.

Figs. 5 and 6 show the phase drop $\Delta\varphi$ on both dc SQUID and bi-SQUID with $i_{c3} = 2$ and the same inductance values $l = 0.25$ (in Fig. 5) and $l = 0.5$ (in Fig. 6) versus the transport current i_b . In all cases, the same dc magnetic flux $\Phi_{dc} = \Phi_0/3$ is applied to the devices. One can see considerable improvement in the linearity attainable for the phase-current dependence $\Delta\varphi(i_b)$ with using bi-SQUIDS. Linear regime becomes now possible for the amplitudes of the current of the signal and idler wave process up to about critical current I_c of the base junctions.

At the same time, it should be noted that the linearity improvement with using of bi-SQUIDS may be accompanied by a slight decrease in the modulation depth m of the effective inductance of the cells at the same magnetic flux applied by the pump

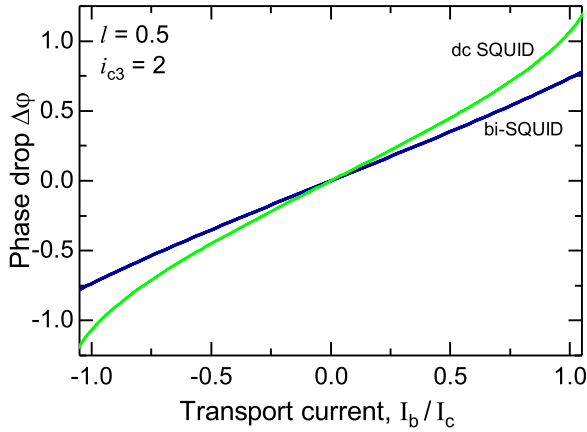


Fig. 6. Phase drops on both dc SQUID (green line) and bi-SQUID (blue line) with $i_{c3} = 2$ and same value $l = 0.5$ versus transport current. The same dc magnetic flux $\Phi_{dc} = \Phi_0/3$ is applied to both devices.

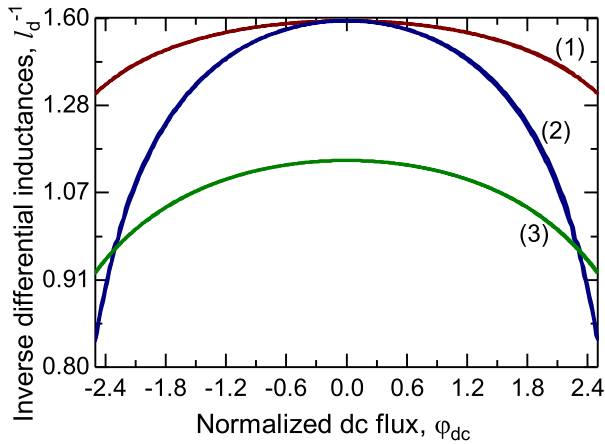


Fig. 7. Normalized inverse differential inductance $(l_d)^{-1}$ versus normalized value of the applied dc magnetic flux $\varphi_{dc} = 2\pi\Phi_{dc}/\Phi_0$ for bi-SQUID with $i_{c3} = I_{c3}/I_c = 2$ and normalized geometric inductance $l = 0.5$ (1) and for dc SQUID with $l = 0.5$ (2) and $l = 1.5$ (3). These data mean that the modulation depth of the effective inductance of bi-SQUID provided by the magnetic flux of the pump signal decreases by 2 to 3 times as compared to dc SQUID.

wave, since the shielding ability of the circuit grows due to the additional current I_3 flowing through the geometric inductance. Such an influence of the added junction can be interpreted as an increase in magnitude of the normalized geometric inductance l . In turn, it reduces the feasible change of the maximum superconducting current under impact of the applied magnetic flux and hence this may decrease modulation depth m of the inverse value of the effective differential inductance.

Fig. 7 shows the calculated inverse differential inductance $(l_d)^{-1} = [d(\Delta\varphi)/d(i_b)]^{-1}$ versus the applied dc magnetic flux $\varphi_{dc} = 2\pi\Phi_{dc}/\Phi_0$ for bi-SQUID with $i_{c3} = 2$ and normalized geometric inductance $l = 0.5$ (1), as well as dc SQUID with $l = 0.5$ (2) and $l = 1.5$ (3). These data mean that the modulation depth m of the inverse differential inductance of bi-SQUID caused by magnetic flux of the pump signal may be decreased by 2 to 3 times as compared to dc SQUID with the same inductive and critical-current parameters. The decrease can be compensated by increase of either the pump wave power

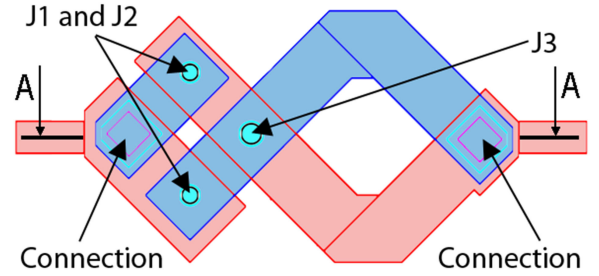


Fig. 8. Layout of the bi-SQUID designed to be used as a cell of the artificial signal transmission line of JTWPA. Two superconductor layers M1 (lower) and M2 (upper) are shown with red and blue colors, respectively.

TABLE I
KEY PARAMETERS OF THE DESIGNED VARIANTS JTWPA

Critical current of the main JJs	$I_c, \mu\text{A}$	5
Ratio of critical currents	I_{c3}/I_c	1.52
Inner dimension of the main square loop	$d, \mu\text{m}$	12
Loop metallization width	$h, \mu\text{m}$	8
Inner size of the small loop	$d_{sm}, \mu\text{m}$	3
Main (geometric) inductance	L, pH	20
3-junction loop inductance	L_{sm}, pH	5
Normalized main (geometric) inductance	l	0.30
Expected differential inductance of bi-SQUID at $\Phi_{dc} \approx \Phi_0/3$	L_d, pH	47
Expected normalized differential inductance of bi-SQUID at $\Phi_{dc} \approx \Phi_0/3$	l_d	0.7
Capacity to ground	C_0, fF	19,7

or the coupling factor $\kappa = M/L_1$, as well as by increase in number of the cells in both the pump and signal transmission lines.

IV. DESIGN OF JTWPA BASED ON NIOBIUM TECHNOLOGY

Fig. 8 shows the developed layout pattern of bi-SQUID to be used as elementary cell of the artificial signal transmission line of JTWPA. The design answers the requirement of minimization of the geometric inductance of the 3-junction loop [17, 18]. To make easier attaining the optimal device parameters $I_{c3}/I_c \approx 1.5$ to 2, $l \approx 0.25$ to 1, the critical current density was chosen to be $j_c \approx 150 \text{ A/cm}^2$ at the area $S \approx 3 \mu\text{m}^2$ of the main junctions J1, J2. The other key parameters of the bi-SQUID and signal line with the cells are given in Table I.

The amplifier is under development to be realized using the fabrication process successfully implemented at IRE RAS [19]. The process is based on using tunnel Nb-AlO_x-Nb Josephson junctions and is compatible with the HYPRES fabrication process [20]. In the fabrication technique, the bi-SQUID cell vertical section along the axial line denoted by two arrows "A" in the cell layout (Fig. 8) is shown schematically in Fig. 9. Table II presents the physical layer process specifications for the fabrication technique capable of providing the layer thickness deviation less than 10%. Using these fabrication process facilities, a variety of superconductor electronic devices, such as integrated receivers [21], Josephson metamaterials [22], dc SQUIDS [23], has been already fabricated with high fidelity.

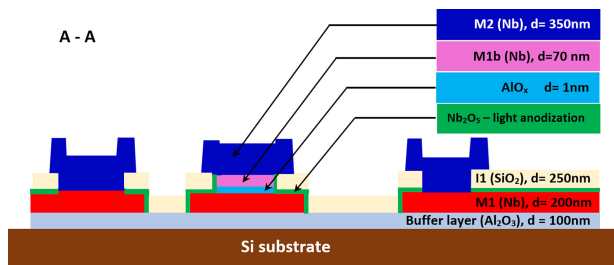


Fig. 9. Schematic profile of the bi-SQUID cell with the layout shown in Fig. 8. The section is done along the axial line denoted by two arrows “A” in the layout. In compliance with Fig. 8, two superconductor layers M1 (lower) and M2 (upper) are shown with red and blue colors, respectively.

TABLE II
PHYSICAL LAYER PROCESS SPECIFICATIONS FOR JTWPA

Layer	Material	Physical layer properties	Thickness nm
-	Al ₂ O ₃	Buffer layer	100
M1	Nb/AlO _x /Nb	Trilayer base electrode, Nb tunnel barrier, AlO _x trilayer counter electrode, Nb	200 7 80
I1		Formation of the tunnel junction region by reactive-ion etching (RIE)	80
		Light anodization; 10 V	20
	SiO ₂	SiO ₂ , insulator. Capacitance: 0.17 fF/μm ² ±25% (Estimation)	250
ETCH		Etching (Nb and AlO _x) for direct contact of M1 to M2 (RIE + KOH)	
M2	Nb	Superconductor layer, Nb,	350
CONT	Al/Au	Contact pads metallization	200
ALO		Final removal of anodization bridges (RIE)	

V. CONCLUSION

A new JTWPA design is proposed to increase the spurious-free dynamic range (SFDR) of the device. For this purpose, dc SQUID is substituted for bi-SQUID as a basic cell of the signal Josephson transmission line to improve linearity of the cell phase-current relation. When using a bi-SQUID, the improvement in linearity is achieved due to the influence of the third Josephson junction, the current through which increases with an increase in the absolute value of the total current of the signal and idler waves and changes division of the current between the main Josephson junctions. This results in reducing of the junction current flowing through that Josephson junction in which the most nonlinear relationship between the current and phase is realized. Such a redistribution of the currents becomes impossible at $I \rightarrow 0$; however, the value of the normalized geometric inductance $l \simeq 0.25$ to 1 is quite sufficient. The effect of improving linearity increases with an increase in the critical current I_{c3} of the third junction and becomes quite sufficient at $i_{c3} = I_{c3} / I_c \simeq 1.5$ to 2.

The first version of the JTWPA with three-wave mixing has been designed; all basic cell elements were modeled, the main parameters of the JTWPA were evaluated.

REFERENCES

- [1] M. Sweeny and R. Mahler, “A travelling-wave parametric amplifier utilizing Josephson junctions,” *IEEE Trans. Magn.*, vol. 21, no. 2, pp. 654–655, Mar. 1985.
- [2] C. Bockstiegel *et al.*, “Development of a broadband NbTiN traveling wave parametric amplifier for MKID readout,” *J. Low Temp. Phys.*, vol. 176, no. 3, pp. 476–482, 2014.
- [3] K. O’Brien, C. Macklin, I. Siddiqi, and X. Zhang, “Resonant phase matching of Josephson junction traveling wave parametric amplifiers,” *Phys. Rev. Lett.*, vol. 113, 2014, Art. no. 157001.
- [4] C. Macklin *et al.*, “A near-quantum-limited Josephson traveling-wave parametric amplifier,” *Science*, vol. 350, no. 6258, pp. 307–310, 2015.
- [5] T. C. White *et al.*, “Traveling wave parametric amplifier with Josephson junctions using minimal resonator phase matching,” *Appl. Phys. Lett.*, vol. 106, no. 24, 2015, Art. no. 242601.
- [6] M. T. Bell and A. Samolov, “Traveling-wave parametric amplifier based on a chain of coupled asymmetric SQUIDs,” *Phys. Rev. Appl.*, vol. 4, no. 2, 2015, Art. no. 024014.
- [7] A. B. Zorin, Josephson “Traveling-wave parametric amplifier with three-wave mixing,” *Phys. Rev. Appl.*, vol. 6, 2016, Art. no. 034006.
- [8] A. B. Zorin, M. Khabipov, J. Dietel, and R. Dolata, “Traveling-wave parametric amplifier based on three-wave mixing in a Josephson metamaterial,” in *Proc. 16th Int. Supercond. Electron. Conf.*, 2017, pp. 1–3.
- [9] M. Haider, J. A. Russer, J. A. Patino, C. Jiruschek, and P. Russer, “A Josephson traveling wave parametric amplifier for quantum coherent signal processing,” in *Proc. IEEE MTT-S Int. Microw. Symp.*, 2019, pp. 956–958.
- [10] A. Miano and O. Mukhanov, “Symmetric traveling-wave parametric amplifier,” *IEEE Trans. Appl. Supercond.*, vol. 29, no. 5, Aug. 2019, Art. no. 1501706.
- [11] A. B. Zorin, “Flux-driven Josephson traveling-wave parametric amplifier,” *Phys. Rev. Appl.*, vol. 12, no. 4, 2019, Art. no. 044051.
- [12] L. Planat *et al.*, “Photonic-crystal Josephson traveling-wave parametric amplifier,” *Phys. Rev. X*, vol. 10, no. 2, 2020, Art. no. 021021.
- [13] A. B. Zorin, “Quasi-phaseshifting in a poled Josephson traveling-wave parametric amplifier with three-wave mixing,” *Appl. Phys. Lett.*, vol. 118, no. 22, 2021, Art. no. 222601.
- [14] Y. M. Blanter and M. Büttiker, “Shot noise in mesoscopic conductors,” *Phys. Rep.*, vol. 336, pp. 1–166, 2000.
- [15] D. Rogovin and D. E. Scalapino, “Fluctuation phenomena in tunnel junctions,” *Ann. Phys.*, vol. 86, pp. 1–90, 1974.
- [16] V. K. Kornev, I. I. Soloviev, N. V. Klenov, and O. A. Mukhanov, “Bi-SQUID: A novel linearization method for dc SQUID voltage response,” *Supercond. Sci. Technol.*, vol. 22, no. 11, 2009, Art. no. 114011.
- [17] V. K. Kornev, N. V. Kolotinskiy, D. E. Bazulin, and O. A. Mukhanov, “High-linearity Bi-squid: Design map,” *IEEE Trans. Appl. Supercond.*, vol. 28, no. 7, Oct. 2018, Art. no. 1601905.
- [18] V. K. Kornev, N. V. Kolotinskiy, and O. A. Mukhanov, “Bi-SQUID: Design for applications,” *Supercond. Sci. Technol.*, vol. 33, no. 11, 2020, Art. no. 113001.
- [19] P. N. Dmitriev, L. V. Filippenko, and V. P. Koshelets, “Applications in superconducting SIS mixers and oscillators: Toward integrated receivers,” in *Josephson Junctions*. Jenny Stanford, pp. 185–244, 2017.
- [20] HYPRES Nb Process Design Rules. Revision 24. Accessed: Jan. 11, 2008. [Online]. Available: <http://www.hypres.com>
- [21] G. de Lange *et al.*, “Development and characterization of the superconducting integrated receiver channel of the TELIS atmospheric sounder,” *Supercond. Sci. Technol.*, vol. 23, no. 4, 2010, Art. no. 045016.
- [22] S. Butz, P. Jung, L. V. Filippenko, V. P. Koshelets, and A. V. Ustinov, “A one-dimensional tunable magnetic metamaterial,” *Opt. Exp.*, vol. 21, no. 19, pp. 22540–22548, 2013.
- [23] E. A. Kostyurina *et al.*, “High-symmetry DC SQUID based on the Nb/AlOx/Nb Josephson junctions for nondestructive evaluation,” *J. Commun. Technol. Electron.*, vol. 62, no. 11, pp. 1306–1310, 2017.